Published online 25 August 2006 *Nucleic Acids Research, 2006, Vol. 34, No. 15* ***4225–4231***
doi:10.1093/nar/gkl452

SURVEY AND SUMMARY

Unraveling helicase mechanisms one molecule at a time

Ivan Rasnik[1], Sua Myong[2] and Taekjip Ha[2,3,*]

[1]Department of Physics, Emory University, Atlanta, GA 30322,USA, [2]Department of Physics, University of Illinois, Urbana, IL 61801, USA and [3]Howard Hughes Medical Institute, Urbana, IL 61801, USA

Received April 1, 2006; Revised May 25, 2006; Accepted June 12, 2006

ABSTRACT

Recent years have seen an increasing number of biological applications of single molecule techniques, evolving from a proof of principle type to the more sophisticated studies. Here we compare the capabilities and limitations of different single molecule techniques in studying the activities of helicases. Helicases share a common catalytic activity but present a high variability in kinetic and phenomenological behavior, making their studies ideal in exemplifying the use of the new single molecule techniques to answer biological questions. Unexpected phenomena have also been observed from individual molecules suggesting extended or alternative functionality of helicases *in vivo*.

INTRODUCTION

Helicases separate double-stranded nucleic acids into the single-stranded intermediates needed for many cellular processes (1). These enzymes are considered motor proteins due to their ability to move along nucleic acids using the chemical energy released from the hydrolysis of ATP or other nucleoside triphosphates. To probe their mechanism at the most fundamental level, one would ideally like to measure real-time structural changes of a helicase–DNA complex during each reaction step. Single-molecule techniques (2–13) are promising for this goal because they can detect the conformational changes and biochemical reactions of individual biomolecules with milliseconds time resolution under biologically relevant solution conditions.

Helicases are molecular machines, characterized by their translocation rates, unwinding rates, physical and kinetic step size, directionality and processivity. There is a wide variability in these parameters among different families and subfamilies. The unwinding reaction in general consists of helicase translocation along double-stranded substrate and its separation into single-strands. This general mechanism has been exploited in many single molecule helicase studies. In contrast, some helicase-catalyzed reactions have unique features that allow for distinctive experimental designs. Examples are Holliday junction branch migration by RuvAB and the multi-subunit protein RecBCD that has both nuclease and helicase activities. Here, we compare different single molecule techniques in terms of their time resolution and base pair resolution in detecting helicase-catalyzed unwinding reaction (summarized in Table 1), and discuss the novel scientific findings from the studies of *Escherichia coli* Rep, RecBCD and RuvAB performed using fluorescence or the tethered particle assay. We refer to an accompanying review (14) for the detailed discussion of helicase studies performed under external force.

FORCE-EXTENSION TECHNIQUES

Force-extension experiments (15,16) can detect changes in the elastic properties of the DNA or RNA substrate, represented in the force-extension curves. By pulling both ends of the substrate via flow, magnetic or optical tweezers, the DNA (or RNA) can be stretched under different applied forces, adding another dimension to the variable space. Strand separation reaction can be detected as a change in the end to end distance of the polymer with up to a few base pair resolution and tens of milliseconds time resolution using optical tweezers and with generally poorer resolution using magnetic tweezers.

Optical tweezers have been used to study the RNA unwinding by NS3, an essential RNA helicase for hepatitis C viral replication (17) belonging to the superfamily 2 (13), and to study RecBCD (10), an enzyme that participates in the repair of chromosomal DNA (18). Magnetic tweezers have been used to study DNA unwinding by the *E.coli* UvrD helicase (8) and branch migration catalyzed by RuvAB (19,20). UvrD is a 3′ to 5′ DNA helicase that belongs to the superfamily 1 and shares extensive sequence similarity (21) and high structural homology (21–23) with Rep and PcrA helicases. RuvAB is involved in the processing of the Holiday junction (24), a key intermediate in homologous recombination. This four way DNA junction (Figure 1c) can undergo spontaneous branch migration if it is made of homologous sequences. RuvAB ensures that branch migration

*To whom correspondence should be addressed. Tel: +1 271 265 0717; Email: tjha@uiuc.edu

occurs efficiently in one direction, shortening two arms and lengthening the other two arms of the junction. By attaching the end of one arm to a microscope slide and a paramagnetic bead to the end of the opposite arm, it is possible to follow the changes in the length of the arms under applied force (19,20).

TETHERED PARTICLE ASSAY

A closely related technique which does not require the use of external forces is the tethered particle assay (25). The fundamental principle here is that the amplitude of the Brownian motion of a bead tethered to a surface through a rigid polymer is related to the length of the polymer. Light microscopy is used to detect the position of the bead, which could be attached to the enzyme (Figure 1a) or the DNA substrate (Figure 1b). Translocation of the enzyme along the substrate or changes in the length of the substrate can be followed. The technique has a low spatial resolution but requires a relatively simple experimental setup and can be a good alternative for investigating various aspects of highly processive enzymes.

Dohoney and Gelles (4) studied RecBCD using this technique. RecBCD combines highly processive and rapid helicase activity with strand specific nuclease activity. Recognition of a specific DNA sequence (χ) switches the polarity of DNA cleavage. By attaching a 200 nm polystyrene bead to the RecD unit they detected the RecBCD movement on a double-stranded (ds) DNA attached to a glass surface at one end (Figure 1a). Translocation was unidirectional at all times and the χ sequence encounter did not eject the bead (hence the RecD unit) although it was not possible to determine whether the χ sequence was recognized by RecBCD due to the limited spatial resolution (~30 nm or ~100 bp) and time resolution (~0.5 s).

Table 1. Time resolution and base pair resolution of single molecule unwinding assays

Technique	Basepair resolution	Time resolution	Helicase studied
Optical trap	2–6 bp	20 ms	RecBCD, NS3
Magnetic tweezers	10–30 bp	0.04–01.0 s	UvrD, RuvAB
TPA	~100 bp	~0.5 s	RecBCD, RuvAB
Microfluidic assay	~200 bp	~0.3 s	RecBCD
Single molecule FRET	<5 bp	15 ms	Rep

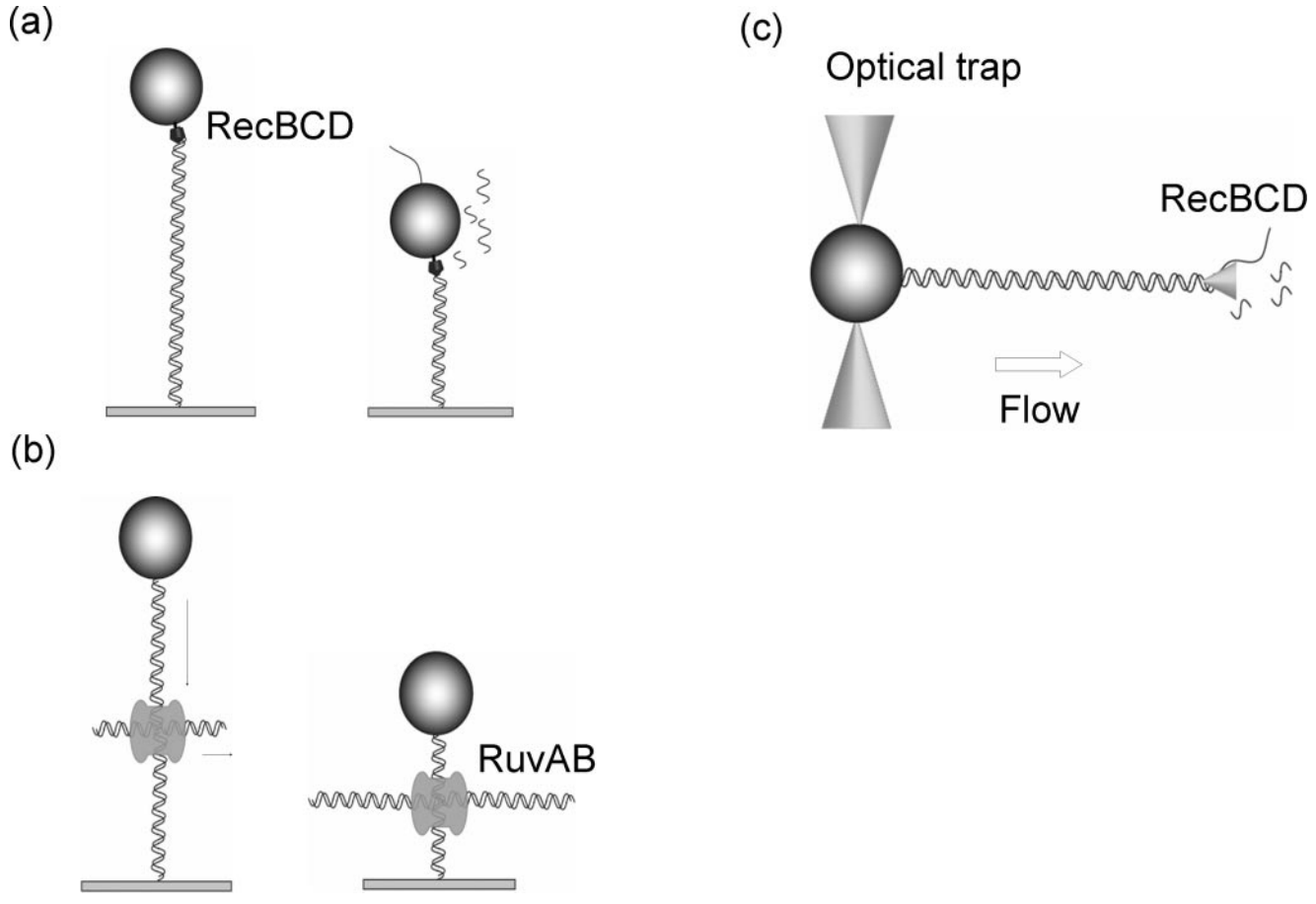

Figure 1. Schematic representations of single molecule helicase assays. (**a**) Tether particle assay (TPA) for RecBCD. The biotin tagged RecD subunit is attached to a streptavidin-coated polystyrene bead and the course of the reaction is followed by measuring the amplitude of the Brownian motion of the bead. (**b**) TPA studies of Holliday junction branch migration catalyzed by RuvAB. The bead is attached to the DNA substrate. Branch migration changes the arm lengths, which can be measured as changes in the bead's Brownian motion. (**c**) Microfludic studies of RecBCD enzymatic reaction. The DNA is attached to a bead that is held in a microfluidic channel by an optical trap. The flow extends the DNA. Fluorescence imaging of the DNA labeled with intercalating dyes measures the contour length of the DNA, which changes as the reaction progresses.

Branch migration catalyzed by RuvAB was also studied using the tethered particle assay (26). The Brownian motion of a polystyrene bead attached to one arm of the junction was used to follow the extent of branch migration (Figure 1b) with a resolution of tens of nanometers. The bead position was recorded at a video rate of 25 frames/s and the amplitude of the Brownian motion was determined by the standard deviation of the bead position over 4 s. A high variability from 7 to 37 bp/s in the reaction rate was observed among different molecules but their average rate was in agreement with studies performed using magnetic tweezers (19,20). Branch migration was impeded when RuvAB encountered a significantly heterologous region (>25 bp), and the probability of overcoming the barrier depended on the degree of heterology and the lifetime of the stalled RuvAB complex.

MICROFLUIDICS

A novel single molecule technique (27) was introduced for the studies of RecBCD. RecBCD degrades the single-strand(s) left behind as it unwinds duplex DNA. This unique behavior was used to monitor the time course of unwinding by fluorescently imaging YOYO dyes intercalated to the duplex DNA. The YOYO fluorescence is lost when the duplex is destroyed and the length of the DNA image obtained using a CCD camera becomes shorter as the reaction progresses. The DNA was stretched via hydrodynamic drag applied in a microfluidic device while one end of the DNA, attached to a polystyrene bead, was held in an optical trap (Figure 1c). A controlled initiation of the reaction was achieved by moving the microfluidic device so that the bead–DNA complex shifts between the two halves of the microfluidic channel with different solution conditions (e.g. ±ATP and/or ±RecBCD). The RecBCD reaction showed the average rate of 900 bp/s (with high variability between single molecules) and processivity up to 42 000 bp. The time resolution was about 0.3 s and the effective spatial resolution was ~3000 bp in the original study. More precise studies later showed that when the enzyme pauses briefly upon encountering the χ sequence and the unwinding speed is reduced by a factor of two on average when the enzyme resumes its movement (9), leading to the proposal that the RecD motor may functionally decouple from the holoenzyme. A variation of the technique where the RecD unit was tagged with a very bright fluorescent bead (11) was used to rigorously confirm the work of Dohoney and Gelles with higher resolution.

SINGLE MOLECULE FRET

A different approach to single molecule studies of helicases comes from the use of single molecule fluorescence resonant energy transfer (smFRET) (28–31). In this technique the distance between fluorescent dyes is determined by the amount of energy transferred from a donor dye to an acceptor dye, which can be experimentally estimated by measuring the intensities of both dyes. Single molecule FRET is unique in that it can measure the internal conformational changes of a single biological molecule, be it DNA or protein, in its center of mass frame. Thus, exquisite distance resolution, <1 nm, can be obtained without the need for ultra-stable experimental environments. In addition, there is great flexibility in where to attach the fluorophore. For example, DNA–DNA FRET with the donor and acceptor both on DNA can measure the changes in DNA conformation (unwinding, stretching, etc) induced by the action of the protein (6), and protein–DNA FRET can detect the binding geometry (7) as well as ATP-powered protein translocation on DNA (12). Furthermore, protein–protein FRET can detect the protein conformational changes that accompany its function (12,32–34). Recent developments in three (or more)-color FRET (35–37) should make it possible to obtain information on more than one distance at a time, enabling the simultaneous measurements of two observables, e.g. DNA unwinding and protein conformational change.

Unwinding kinetics

Single molecule FRET technique has been applied to measure structural changes of the DNA upon the action of *E.coli* Rep helicase to detect DNA unwinding with $\leqslant$10 bp resolution (6). The substrate used was an 18 bp duplex with a 3′-$(dT)_{20}$ tail with a donor (Cy3) and an acceptor (Cy5) fluorophore attached to the single-stranded (ss)/dsDNA junction (Figure 2a). DNA molecules were specifically immobilized to a PEG surface and imaged using a total internal reflection fluorescence microscope. A solution containing both Rep and ATP was delivered and while the unwinding time records were being recorded via FRET. Before unwinding begins, the distance, R, between the two dyes is small ($E \sim 1$; $E \equiv 1/[1 + I_D/I_A]$ is an approximation for FRET efficiency $= 1/[1 + (R/R_0)^6]$, where I_D and I_A are intensities for donor and acceptor, respectively and $R_0 \sim$ 5–6 nm). As the DNA is unwound, the time-averaged R increases (E decreases). If the DNA is fully unwound, the donor strand diffuses away from the surface and the fluorescence signal abruptly disappears, clearly marking the completion of unwinding (Figure 2a and b).

Linear protein concentration dependence for unwinding initiation above 20 nM protein was observed, which might be interpreted as evidence that a Rep monomer can unwind DNA. However, experiments using a DNA substrate fluorescently labeled at near extremities indicated that a Rep monomer binds to the DNA with a few nanomolar affinity and the monomer binding is already saturated at 20 nM Rep (6). Therefore, the Rep concentration-dependent unwinding initiation rate probably reflects the requirement of another monomer to bind to the existing monomer–DNA complex (6,38). Unwinding experiment using a 40 bp duplex DNA were also carried out (6). In contrast to 18 bp duplex, unwinding of 40 bp led to frequent stalls that lasted for a few seconds, either leading to DNA rewinding (FRET returns to 100%) or unwinding restart and completion. The unwinding restart required free Rep molecules in solution, leading to the proposal that the unwinding stalls when the active helicase complex dissociates, leaving a monomer on the DNA, and that the rewinding is observed if the remaining monomer dissociates. The unwinding can be restarted if an additional helicase monomer(s) binds to the stalled monomer.

Protein–DNA complex conformations

As mentioned before, smFRET can be used to obtain structural information of biomolecular complexes. Single cysteine

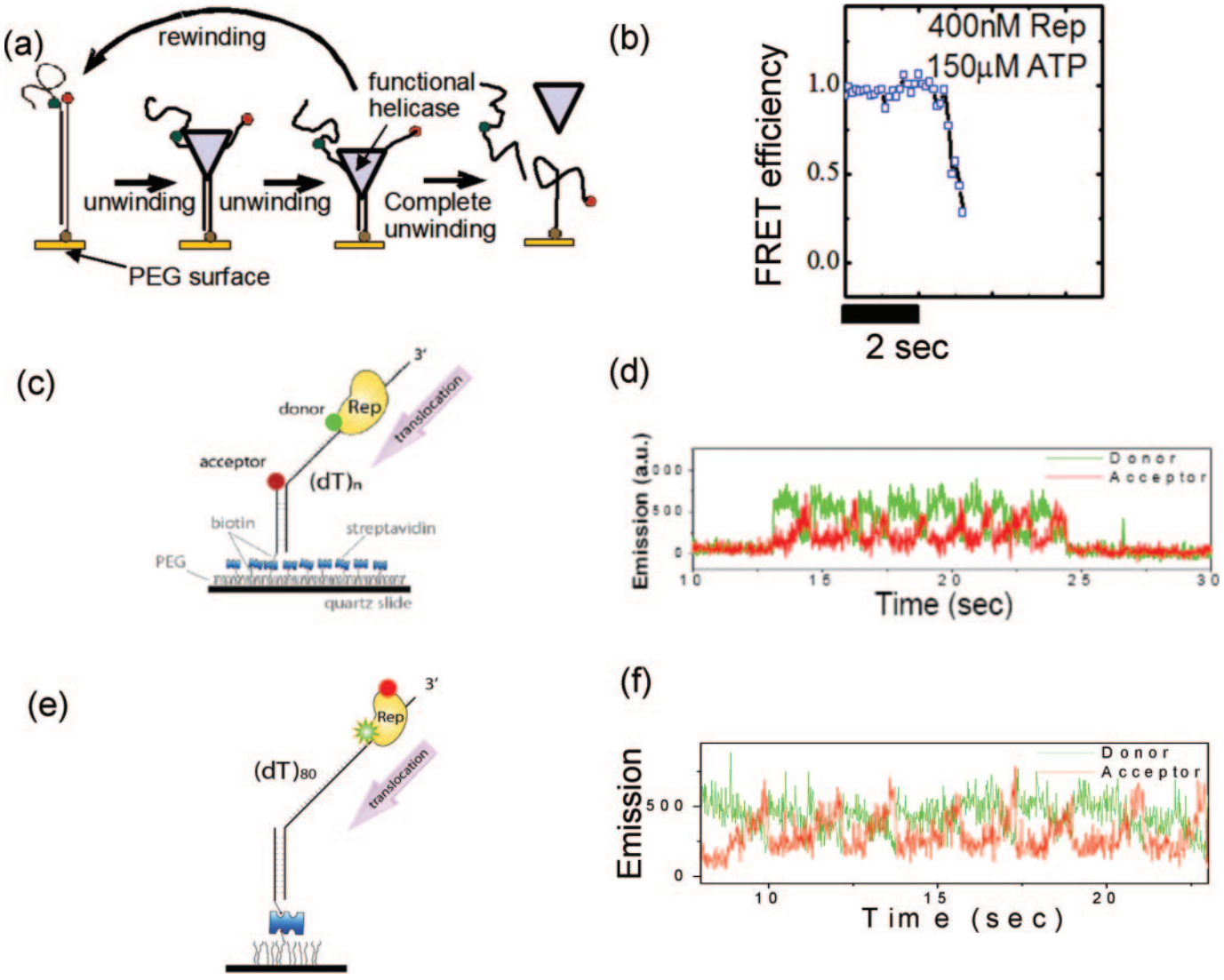

Figure 2. Single molecule FRET experiements with Rep helicase. (**a**) Schematic representation of the unwinding reaction catalyzed by Rep. The distance between donor and acceptor dyes at the junction indicates the extent of the reaction. If the protein complex dissociates before the reaction is completed the DNA can rezip again. When the reaction is completed the donor strand dissociates form the surface giving clear indication that the reaction was completed. (**b**) Typical FRET efficiency time trace for an individual molecule that completed the reaction. The reaction initiation time (observed as the time before the FRET efficiency starts to decrease) depends on the protein concentration. (**c**) FRET between a donor attached to a Rep monomer and an acceptor on the DNA reports on the translocation of Rep on ssDNA. (**d**) Typical time traces (donor in green and acceptor in red) for the translocation of Rep on ssDNA. Multiple cycles are clearly observed indicating a repetitive shuttling behavior. The fluorescence intensity is negligible before protein binding and it disappears after protein dissociation or photobleaching. (**e**) Same experiment but donor and acceptor dyes are both located on different domains of the protein. (**f**) Time traces of donor and acceptor dyes show that the 2B domain of the protein undergoes conformational changes correlated with the translocation of the helicase on the ssDNA. Adapted from Ha *et al*., 2002 and Myong *et al*., 2005. Copyright 2002, 2005 Nature Publishing Group.

mutants of Rep that retain activities *in vitro* and *in vivo* were engineered and FRET between a donor on the protein and an acceptor on DNA was measured both in ensemble and in single molecules (7).

Rep and PcrA consist of four major domains called 1A, 2A, 1B and 2B. Crystal structures of Rep bound to ssDNA show two dramatically different Rep monomer conformations ('open' and 'closed') that differ from each other by a large reorientation (130° swiveling) of the 2B domain while the other domains remain essentially unchanged (21). The crystal structure of a PcrA monomer in complex with a partial duplex DNA (dsDNA with a short 3′ ssDNA tail) is found in the closed form (22).

Eight labeling sites were chosen, distributed strategically among all four subdomains. Based on the Rep crystal structure in complex with $(dT)_{16}$ (21), three of these sites were predicted to be closer to the 3′ end of the ssDNA while three others are predicted to be closer to the 5′ end of the ssDNA, and thus also predicted to be closer to the partial duplex junction of the DNA used in this study. The two sites on the flexible 2B domain were also chosen to deduce the orientation of the 2B subdomain relative to both the DNA as well as the remainder of the Rep protein (open or closed).

Both bulk solution and single molecule measurements showed relative Rep orientations consistent with the crystal structures. Furthermore, single molecule measurements

showed that the binding orientation is definitive, i.e. there is not a detectable amount of complexes with the reverse binding orientation.

For each of the eight mutants with a single cysteine at different locations, FRET from a donor on the protein and an acceptor attached to the junction of a partial duplex DNA with a 3′-$(dT)_{20}$ tail was measured in the absence of ATP. Through a triangulation process of the distance constraints obtained from FRET values, it was concluded that the 2B domain is most likely in the closed conformation when a Rep monomer is bound to a partial duplex DNA, similar to the crystal structure of PcrA bound to such a DNA.

ssDNA translocation: kinetics and conformation

To probe ssDNA translocation directly at the single molecule level, single cysteine mutants of Rep were labeled with the donor fluorophore (Cy3) and the movement of a donor-labeled Rep on an acceptor (Cy5)-labeled DNA was detected via single molecule FRET (12). An 18 bp dsDNA with a 3′-$(dT)_{80}$ tail and with a Cy5 attached to the junction was tethered at the duplex end to a polymer-coated quartz slide via biotin-streptavidin and single molecule data were obtained in the presence of 300 pM of Rep and 1 mM ATP in solution using wide-field total internal reflection fluorescence microscopy with 15 ms time resolution (Figure 2c).

When a donor-labeled Rep monomer binds the partial duplex DNA with a 3′ ssDNA tail, the donor fluorescence signal rises abruptly, combined with a weak acceptor signal. This is followed by a gradual decrease in donor signal and a gradual increase in acceptor signal (and corresponding FRET increase), consistent with ssDNA translocation in the 3′ to 5′ direction toward the junction. Since Rep cannot unwind duplex DNA as a monomer *in vitro* (6,38), the junction presents itself as a blockade at which the protein is expected to stop and dissociate. Instead of the anticipated dissociation, what was observed was an instantaneous (within 15 ms) FRET decrease to near the initial value followed by further cycles of a gradual FRET increase and an abrupt FRET decrease (Figure 2d). This sawtooth-like cycle was repeated several times until it finally terminated by protein dissociation or photobleaching.

The sawtooth pattern was interpreted as reflecting repeated cycles of ssDNA translocation followed by the protein snapback to near its initial binding region, termed 'repetitive shuttling'. This data and additional experiments with other substrates provided a possible reason why a Rep monomer is unable to unwind DNA. Whether a helicase unwinds DNA actively or passively, it needs to stay at the junction between dsDNA and ssDNA to exert maximal effects (39). A Rep monomer, however, appears to snap back when it encounters a dsDNA. Similar sawtooth patterns were observed on ssDNA bounded by a stalled replication fork and an Okazaki fragment analogue and it was shown that Rep can interfere with RecA filament formation on ssDNA (12). It is possible that one of the *in vivo* functions of Rep is to shuttle repetitively on ssDNA, thereby keeping it clear of unwanted proteins.

The structural aspects of the repetitive shuttling were also explored using single molecule FRET. Similar to the PcrA bound to a 3′-tailed dsDNA that was crystallized in the closed form (22), it was shown earlier that Rep bound to a 3′-tailed dsDNA in solution favors the closed form (7). To test if the 2B subdomain closes as Rep approaches the junction; a double cysteine mutant of Rep was engineered (positions 97 and 473 on 1B and 2B subdomains, respectively) and was labeled stochastically with Cy3 and Cy5 so that a 2B closing would result in a FRET increase (Figure 2e). Single molecule measurements could identify this mutant labeled with one donor and one acceptor as it moves on an unlabeled DNA with a 3′-$(dT)_{80}$ tail. A representative time trace in Figure 2f shows several cycles of gradual FRET increase and an abrupt FRET decrease. The 2B subdomain closes gradually as the protein approaches a blockade and its complete closing may correlate with the affinity enhancement of the secondary binding site toward the 3′ end of the ssDNA, followed by the snapback and the restart of translocation. The detailed microscopic origin behind the gradual 2B closing is not clear, but it is possible that the 2B movement is a molecular beacon that reports on the more subtle conformations changes that occur within the protein.

CONCLUSION AND OUTLOOK

Comparing single molecule techniques

In this review, we have discussed several single molecule helicase assays. Table 1 summarizes the base pair resolution and time resolution of different techniques in measuring the single molecule unwinding reaction. Techniques such as tethered particle assay and microfluidics are more suitable for studying highly processive enzymes because of their limited spatial resolution. SmFRET and optical tweezers provide in principle the highest possible temporal (milliseconds) and spatial (a few bp) resolution. SmFRET is relatively insensitive to the mechanical noise since it reports on the internal motions within the center of mass frame of the system under study. However, because the distance range that can be probed by FRET is between $\sim$2 and 8 nm, smFRET cannot be used to measure the extended movements of a highly processive helicase. Other single molecule techniques do not have such limitation on the dynamic range but because they measure the motion in the laboratory frame, mechanical noises and thermal drift have to be dealt with. Using the external force as an additional knob is very useful in understanding the mechanochemistry of motor proteins, but the functional parameters at the zero force limit can be obtained only through extrapolation because the resolution deteriorates when the force is reduced.

Comparing single molecule and bulk studies

Researchers design and carry out single molecule measurements because such studies in principle can reveal novel properties that cannot be observed in bulk. That is, some of the most interesting and surprising discoveries made from single molecule studies cannot be confirmed by repeating the measurement in bulk. How can we then be sure that the single molecule measurements themselves do not introduce artifacts, e.g. due to fluorescent labeling, tethering to the surface or bead or applied force? The best one can do is to

compare parameters that can be measured both at the single molecule and ensemble level to ascertain that at least the average behavior of single molecules is identical or highly similar to that determined in bulk. Single molecule studies of RecBCD, Rep and RuvAB showed that the speed and processivity of unwinding and branch migration were not altered. Interestingly, the single molecule UvrD studies revealed much faster and much more processive DNA unwinding (8) than in the bulk studies (40). As efficient unwinding by UvrD was observed only at high forces (8), the discrepancy was attributed to the force which is absent in the bulk studies (41). The applied force may have altered the energy landscape for the unwinding reaction so that a UvrD monomer can unwind the DNA at the speed of ssDNA translocation, instead of a required dimer in the absence of force (41). Similarly, it was proposed that a monomer of NS3 was responsible for RNA unwinding under applied force (17) in contrast to the dimer-based unwinding observed in bulk (42). This may have been responsible for the discrepancy in the step sizes of unwinding by NS3 (11 versus 18 bp in single molecule and bulk studies, respectively).

The power of single molecule approaches

Analysis of ensemble kinetic data often requires assumptions on the kinetic behavior of individual molecules. For example, the kinetic unwinding step sizes of UvrD (43), T7 helicase (44), RecBCD (45) and NPH-II (46) were deduced under the assumption that all individual molecules in a given experiment possess the same reaction rate. Such an assumption can be validated only via single molecule measurements. Interestingly, the single molecule branch migration analysis of RuvAB revealed a series of discrete migration rates suggesting that different numbers of functional units may be involved in the process (26). In the case of RecBCD, both optical trap (10) and microfluidic (27) analysis revealed a great variability in unwinding rate between single RecBCD molecules. Although strong proof that such variability is intrinsic to the enzyme itself is still lacking, this type of molecular heterogeneity can in principle complicate the interpretation of the ensemble kinetic measurements. For example, unwinding speed reduction by RecBCD after a brief pause at the χ sequence (9) would be impossible to detect in ensemble kinetic studies if there exists a large heterogeneity in unwinding rate. This is because even after the synchronous initiation of unwinding reaction, these molecules would quickly lose synchrony due to the different unwinding rates. Whether the observed molecular heterogeneity has any functional consequences is yet to be determined. It is also tempting to speculate on the biological implications of the many surprising and unexpected discoveries afforded by single molecule approaches. For example, the strand switching behavior of UvrD (8) and repetitive shuttling of Rep (12) may imply that these proteins can have alternative functions that do not require strand separation. Finally, the optical trap studies on RNA unwinding by NS3 (17) detected individual steps at two different levels, termed steps and substeps, which marks the first direct detection of stepping by any helicase. These steps occur in a stochastic manner and would have been washed out if the trajectories were averaged over many molecules.

Despite rapid progress made on various fronts including biochemistry, genetics and structural biology, many fundamental questions about helicases remain largely unanswered. What is the origin of directionality in nucleic acids translocation and unwinding? What are the step sizes of unwinding and translocation and how many layers are there in the hierarchy of steps? How many ATP are consumed per step? Is unwinding passive or active? How is ATP hydrolysis coupled into mechanical movement? How do helicases function in relation to other proteins? Surely, single molecule approaches will play an important role in future endeavors of the community in unraveling the mechanistic details.

ACKNOWLEDGEMENTS

The authors thank Kaushik Ragunathan for carefully reading the manuscript. The funding for the single molecule FRET studies reviewed here was provided by the National Institutes of Health (GM065367). Funding to pay the Open Access publication charges for this article was provided by the National Institutes of Health.

Conflict of interest statement. None declared.

REFERENCES

1. Lohman,T.M. and Bjornson,K.P. (1996) Mechanisms of helicase-catalyzed DNA unwinding. *Annu. Rev. Biochem.*, **65**, 169–214.
2. Weiss,S. (1999) Fluorescence spectroscopy of single biomolecules. *Science*, **283**, 1676–1683.
3. Moerner,W.E. and Orrit,M. (1999) Illuminating single molecules in condensed matter. *Science*, **283**, 1670–1676.
4. Dohoney,K.M. and Gelles,J. (2000) Single molecule studies of the RecBCD DNA helicase. *Biophys. J.*, **78**, 262A–262A.
5. Bianco,P.R., Brewer,L.R., Corzett,M., Balhorn,R., Yeh,Y., Kowalczykowski,S.C. and Baskin,R.J. (2001) Processive translocation and DNA unwinding by individual RecBCD enzyme molecules. *Nature*, **409**, 374–378.
6. Ha,T., Rasnik,I., Cheng,W., Babcock,H.P., Gauss,G.H., Lohman,T.M. and Chu,S. (2002) Initiation and re-initiation of DNA unwinding by the *Escherichia coli* Rep helicase. *Nature*, **419**, 638–641.
7. Rasnik,I., Myong,S., Cheng,W., Lohman,T.M. and Ha,T. (2004) DNA-binding orientation and domain conformation of the *E.coli* Rep helicase monomer bound to a partial duplex junction: single-molecule studies of fluorescently labeled enzymes. *J. Mol. Biol.*, **336**, 395–408.
8. Dessinges,M.N., Lionnet,T., Xi,X.G., Bensimon,D. and Croquette,V. (2004) Single-molecule assay reveals strand switching and enhanced processivity of UvrD. *Proc. Natl Acad. Sci. USA*, **101**, 6439–6444.
9. Spies,M., Bianco,P.R., Dillingham,M.S., Handa,N., Baskin,R.J. and Kowalczykowski,S.C. (2003) A molecular throttle: the recombination hotspot chi controls DNA translocation by the RecBCD helicase. *Cell*, **114**, 647–654.
10. Perkins,T.T., Li,H.W., Dalal,R.V., Gelles,J. and Block,S.M. (2004) Forward and reverse motion of single RecBCD molecules on DNA. *Biophys. J.*, **86**, 1640–1648.
11. Handa,N., Bianco,P.R., Baskin,R.J. and Kowalczykowski,S.C. (2005) Direct visualization of RecBCD movement reveals cotranslocation of the RecD motor after Chi recognition. *Mol. Cell*, **17**, 745–750.
12. Myong,S., Rasnik,I., Joo,C., Lohman,T.M. and Ha,T. (2005) Repetitive shuttling of a motor protein on DNA. *Nature*, **437**, 1321–1325.
13. Dumont,S., Cheng,W., Serebrov,V., Beran,R.K., Tinoco,I., Pyle,A.M. and Bustamante,C. (2006) RNA translocation and unwinding mechanism of HCVNS3 helicase and its coordination by ATP. *Nature*, **439**, 105–108.
14. Lionnet,T., Dawid,A., Bigot,S., Barre,F.-X., Saleh,O.A., Heslot,F., Allemand,J.-F., Bensimon,D. and Croquette,V. (2006) DNA mechanics

as a tool to probe helicase and translocase activity. *Nucleic Acids Res*., **34**, doi:10.1093/nar/gkl451.
15. Allemand,J.F., Bensimon,D. and Croquette,V. (2003) Stretching DNA and RNA to probe their interactions with proteins. *Curr. Opin. Struct. Biol*., **13**, 266–274.
16. Bustamante,C., Macosko,J.C. and Wuite,G.J.L. (2000) Grabbing the cat by the tail: manipulating molecules one by one. *Nature Rev. Mol. Cell. Biol*., **1**, 130–136.
17. Kolykhalov,A.A., Mihalik,K., Feinstone,S.M. and Rice,C.M. (2000) Hepatitis C virus-encoded enzymatic activities and conserved RNA elements in the 3′ nontranslated region are essential for virus replication *in vivo*. *J. Virol*., **74**, 2046–2051.
18. Kuzminov,A. (1999) Recombinational repair of DNA damage in *Escherichia coli* and bacteriophage lambda. *Microbiol. Mol. Biol. Rev*., **63**, 751–813.
19. Amit,R., Gileadi,O. and Stavans,J. (2004) Direct observation of RuvAB-catalyzed branch migration of single Holliday junctions. *Proc. Natl Acad. Sci. USA*, **101**, 11605–11610.
20. Dawid,A., Croquette,V., Grigoriev,M. and Heslot,F. (2004) Single-molecule study of RuvAB-mediated Holliday-junction migration. *Proc. Natl Acad. Sci. USA*, **101**, 11611–11616.
21. Korolev,S., Hsieh,J., Gauss,G.H., Lohman,T.M. and Waksman,G. (1997) Major domain swiveling revealed by the crystal structures of complexes of *E.coli* Rep helicase bound to single-stranded DNA and ADP. *Cell*, **90**, 635–647.
22. Velankar,S.S., Soultanas,P., Dillingham,M.S., Subramanya,H.S. and Wigley,D.B. (1999) Crystal structures of complexes of PcrA DNA helicase with a DNA substrate indicate an inchworm mechanism. *Cell*, **97**, 75–84.
23. Subramanya,H.S., Bird,L.E., Brannigan,J.A. and Wigley,D.B. (1996) Crystal structure of a DExx box DNA helicase. *Nature*, **384**, 379–383.
24. Shinagawa,H. and Iwasaki,H. (1996) Processing the holliday junction in homologous recombination. *Trends Biochem. Sci*., **21**, 107–111.
25. Schafer,D.A., Gelles,J., Sheetz,M.P. and Landick,R. (1991) Transcription by single molecules of RNA-polymerase observed by light-microscopy. *Nature*, **352**, 444–448.
26. Dennis,C., Fedorov,A., Kas,E., Salome,L. and Grigoriev,M. (2004) RuvAB-directed branch migration of individual Holliday junctions is impeded by sequence. *EMBO J*., **23**, 2413–2422.
27. Bianco,P.R., Brewer,L.R., Corzett,M., Balhorn,R., Yeh,Y., Kowalczykowski,S.C. and Baskin,R.J. (2000) Processive translocation and DNA unwinding by individual RecBCD enzyme molecules. *Mol. Biol. Cell*, **11**, 438A–438A.
28. Ha,T., Enderle,T., Ogletree,D.F., Chemla,D.S., Selvin,P.R. and Weiss,S. (1996) Probing the interaction between two single molecules: fluorescence resonance energy transfer between a single donor and a single acceptor. *Proc. Natl Acad. Sci. USA*, **93**, 6264–6268.
29. Ha,T. (2001) Single-molecule fluorescence resonance energy transfer. *Methods*, **25**, 78–86.
30. Ha,T.J. (2004) Structural dynamics and processing of nucleic acids revealed by single-molecule spectroscopy. *Biochemistry*, **43**, 4055–4063.
31. Rasnik,I., McKinney,S.A. and Ha,T. (2005) Surfaces and orientations: much to FRET about? *Acc. Chem. Res*., **38**, 542–548.
32. Diez,M., Zimmermann,B., Borsch,M., Konig,M., Schweinberger,E., Steigmiller,S., Reuter,R., Felekyan,S., Kudryavtsev,V., Seidel,C.A. *et al*. (2004) Proton-powered subunit rotation in single membrane-bound F0F1-ATP synthase. *Nature Struct. Mol. Biol*., **11**, 135–141.
33. Margittai,M., Widengren,J., Schweinberger,E., Schroder,G.F., Felekyan,S., Haustein,E., Konig,M., Fasshauer,D., Grubmuller,H., Jahn,R. *et al*. (2003) Single-molecule fluorescence resonance energy transfer reveals a dynamic equilibrium between closed and open conformations of syntaxin 1. *Proc. Natl Acad. Sci. USA*, **100**, 15516–15521.
34. Brasselet,S., Peterman,E.J.G., Miyawaki,A. and Moerner,W.E. (2000) Single-molecule fluorescence resonant energy transfer in calcium concentration dependent cameleon. *J. Phys. Chem. B*, **104**, 3676–3682.
35. Heilemann,M., Tinnefeld,P., Mosteiro,G.S., Parajo,M.G., Van Hulst,N.F. and Sauer,M. (2004) Multistep energy transfer in single molecular photonic wires. *J. Am. Chem. Soc*., **126**, 6514–6515.
36. Hohng,S., Joo,C. and Ha,T. (2004) Single-molecule three-color FRET. *Biophys. J*., **87**, 1328–1337.
37. Clamme,J.P. and Deniz,A.A. (2005) Three-color single-molecule fluorescence resonance energy transfer. *Chemphyschem*., **6**, 74–77.
38. Cheng,W., Hsieh,J., Brendza,K.M. and Lohman,T.M. (2001) *E.coli* Rep oligomers are required to initiate DNA unwinding *in vitro*. *J. Mol. Biol*., **310**, 327–350.
39. Betterton,M.D. and Julicher,F. (2005) Velocity and processivity of helicase unwinding of double-stranded nucleic acids. *J. Phys. Condens. Matter*, **17**, S3851–S3869.
40. Maluf,N.K., Fischer,C.J. and Lohman,T.M. (2003) A dimer of *Escherichia coli* UvrD is the active form of the helicase *in vitro*. *J. Mol. Biol*., **325**, 913–935.
41. Fischer,C.J., Maluf,N.K. and Lohman,T.M. (2004) Mechanism of ATP-dependent translocation of *E.coli* UvrD monomers along single-stranded DNA. *J. Mol. Biol*., **344**, 1287–1309.
42. Serebrov,V. and Pyle,A.M. (2004) Periodic cycles of RNA unwinding and pausing by hepatitis C virus NS3 helicase. *Nature*, **430**, 476–480.
43. Ali,J.A. and Lohman,T.M. (1997) Kinetic measurement of the step size of DNA unwinding by *Escherichia coli* UvrD helicase. *Science*, **275**, 377–380.
44. Jeong,Y.J., Levin,M.K. and Patel,S.S. (2004) The DNA-unwinding mechanism of the ring helicase of bacteriophage T7. *Proc. Natl Acad. Sci. USA*, **101**, 7264–7269.
45. Lucius,A.L., Vindigni,A., Gregorian,R., Ali,J.A., Taylor,A.F., Smith,G.R. and Lohman,T.M. (2002) DNA unwinding step-size of *E.coli* RecBCD helicase determined from single turnover chemical quenched-flow kinetic studies. *J. Mol. Biol*., **324**, 409–428.
46. Jankowsky,E., Gross,C.H., Shuman,S. and Pyle,A.M. (2000) The DExH protein NPH-II is a processive and directional motor for unwinding RNA. *Nature*, **403**, 447–451.